

Inhibition of BK channels by nanomolar concentrations of Ag⁺

Yu Zhou, Xiaoming Xia, Christopher J. Lingle

*Department of Anesthesiology, Washington University School of Medicine, St.
Louis, Missouri*

Running title: Inhibition of BK channels by Ag⁺

Address correspondence to: Dr. Yu Zhou, Department of Anesthesiology,
Washington University School of Medicine, St. Louis, MO 63110. E-mail:
zhouy@morpheus.wustl.edu

Number of pages: 36

Number of tables: 1

Number of figures: 8

Number of references: 41

Number of references: 43

Number of words in the *Abstract*: 156

Number of words in the *Introduction*: 486

Number of words in the *Discussion*: 1259

Abbreviations: KMSF, potassium methanesulfonate; MTSET, [2-(trimethylammonium)ethyl] methanethiosulfonate bromide; MTSES, sodium (2-sulfanatoethyl) methanethiosulfonate; NEM, N-ethylmaleimide; TBA, Tetrabutylammonium nitrate; DTT, dithiothreitol; MTS, methanethiosulfonate; DEPC, diethyl pyrocarbonate; G-V, conductance-potential; V_h, potential for half-maximal activation; BK, large conductance Ca²⁺-activated K⁺ channel; AMG, autometallographic;

Abstract

Silver has been widely used in various medical products due to its antibacterial properties. However, there is only limited information concerning silver-related cytotoxicity. In this study we show that Ag^+ at low nanomolar concentrations (< 10 nM) strongly inhibits the activity of BK channels (Slo1), a widely expressed and physiologically important potassium channel. The Ag^+ inhibition is caused by irreversible modification on cytosolically accessible parts of the BK channel. At least four intracellular cysteines are involved in this process. In addition, at least one of these key cysteines is not accessible to the bulkier thiolate-active reagent MTSET. One of the cys-less construct generated in this study shows gating properties similar to wild type BK channel, but with much lower Ag^+ sensitivity, in which the Ag^+ modification rate was decreased by about 20-fold. The results from the present study suggest a possible contribution of BK channel inhibition to the cytotoxicity of Ag^+ in humans and other species.

Introduction

The bactericidal properties of free Ag^+ have been recognized for more than 3000 years (Russell and Hugo, 1994) and continue to be exploited in a variety of medical applications (Chopra, 2007). However, the potential cytotoxicity of Ag^+ has not been adequately understood even though there have been a number of reports on Ag^+ -related cytotoxicity and neuropathy (Bayston et al., 2007). For example, a medical emergency resulting from acute intoxication with a large dose of Ag^+ was characterized by symptoms such as diarrhea, cardiovascular collapse, convulsions and coma (Dreisbach, 1974). Neuropathy has also been reported from excessive use of silver sulphadiazine or silver absorption from bone cement (Payne et al., 1992; Vik et al., 1985). In addition, experiments in rats have demonstrated that Ag^+ causes functional impairment and axonal loss in the sciatic nerve (Wachter et al., 2002) and decreases the volume of the pyramidal cell layer in the developing hippocampus (Rungby et al., 1987). Therefore it is particularly important to understand the mechanism and molecular targets of Ag^+ cytotoxicity.

There is evidence that Ag^+ can accumulate in nervous system structures and other excitable cells (Stoltenberg et al., 1994; Danscher, 1981; Rungby, 1990). However, the low solubility of AgCl will keep Ag^+ at nanomolar levels on both sides of the cell membrane even under the most toxic conditions. Although a variety of cytosolic proteins have been reported to be sensitive to Ag^+ (Wagner et al., 1975; Hultberg et al., 1997), it is not clear whether Ag^+ at low nanomolar concentrations would induce cytotoxicity by modifying these proteins.

For ion channel biophysicists, given the strong activity of Ag^+ on thiolate groups and similarity in atomic size between Ag^+ and K^+ , Ag^+ has been exploited as a tool in conjunction with cysteine substitution to dissect information regarding accessibility of cysteine-substituted residues in narrow portions of ion channels. Typically, such accessibility studies require either that the wild type channel be resistant to any effects of Ag^+ application, such as P2X2 and CNG channels (Contreras et al., 2008; Li et al., 2008), or that background mutations be made such that Ag^+ sensitivity of the wild type construct is eliminated, such as Shaker channels (del Camino and Yellen, 2001). In general, these cases suggest that, of the ion channels that have been studied in this way, none would be vulnerable to Ag^+ at nanomolar concentrations. However, ion channels differ considerably in the constellation of residues that might be vulnerable to irreversible modification of Ag^+ , such that perhaps some ion channels might be modified during Ag^+ toxicity. Consistent with this possibility, here we report that cytosolic Ag^+ at nanomolar concentrations irreversibly inhibits the large-conductance Ca^{2+} -activated BK-type channels. We further show that at least four cytosolic cysteines are involved in Ag^+ inhibition. One of the cys-less BK constructs generated during this study shows remarkably reduced Ag^+ sensitivity, which may be used as a background construct for cysteine accessibility studies in BK channels when Ag^+ is required as the probe.

Material and Methods

Mutagenesis and Channel Expression

Mutations were induced into the wild-type mouse Slo1 gene (mSlo1) (Butler et al., 1993) with methods described before (Xia et al., 2002). cRNA for oocyte injection was synthesized with SP6 RNA polymerase after DNA was linearized with M1ul. 0.01 – 0.1 ng of cRNA was injected into stage IV *Xenopus* oocytes for channel expression. Recording was performed 2-7 days after injection.

Electrophysiology and Data Analysis

Unless otherwise stated, potassium currents were recorded from excised patches in the inside-out configuration (Hamill et al., 1981). The access resistance of recording electrodes was in the range of 0.8 to 2 M Ω after fire polishing and filling with pipette solution (extracellular side for inside-out patches) containing (in mM): 140 potassium methanesulfonate (KMSF), 20 KOH, 10 HEPES, 2 MgCl₂ (pH 7.0). Ca²⁺ and reagents were applied onto patches (intracellular side for inside-out patches) through bath solution using an SF-77B fast perfusion stepper system (Warner Instruments, Hamden, CT). The standard bath solution (cytosolic side of patch) contained (in mM): 140 KMSF, 20 KOH, 10 HEPES (pH 7.0). Solutions with various [Ca²⁺] were prepared as described before (Zhang et al., 2001). Solutions for Ag⁺ modification were either fluoride-based or nitrate-based, containing (in mM): 10 HEPES, 10 EDTA and 160 KF or KNO₃, respectively (pH 7.0). AgF or AgNO₃ was added before recording to achieve desired free [Ag⁺]. The required [Ag⁺] was calculated by a script written

in Maple 7 (Waterloo Maple Inc., Waterloo, ON, Canada) with equilibrium constants from the National Institute of Standards and Technology Database 46 Version 8.0 (NIST Standard Reference Data, Gaithersburg, MD). The values calculated by this script agree with the results from previous studies (Contreras et al., 2008; del Camino and Yellen, 2001). Before each experiment, the Ag^+ stock solution was diluted into cytosolic media to result in a total of 52.5, 21, 5.25, 2.1, 0.52 μM AgF or AgNO_3 , yielding free $[\text{Ag}^+]$ of 520, 200, 52, 20, 5.2 nM, respectively. Because EDTA also chelates with Ca^{2+} , all Ag^+ modification experiments were performed in Ca^{2+} -free solution to avoid changes in free $[\text{Ag}^+]$. For experiments using [2-(trimethylammonium)ethyl] methanethiosulfonate bromide (MTSET), aliquots of stock solution were thawed and diluted to the desired concentration in bath solution right before application.

Currents were recorded with an Axopatch 200B amplifier (Molecular Devices, Union City, CA) and low-pass filtered at 10 kHz with its 4 pole Bessel filter. Signals were digitized with Digidata 1322A data acquisition system (Molecular Devices) at 100 kHz. The recordings were controlled by the pClamp 9.2 software suite (Molecular Devices). All experiments were performed at room temperature (21-24 $^{\circ}\text{C}$).

Single channel data were analyzed with pClamp 9.2. Macroscopic currents were pre-processed for series resistance correction and capacitive transient subtraction using scripts written in Matlab R11 (MathWorks, Natick, MA) before further analysis. The conductance-potential (G-V) relationship of BK currents was constructed from isochronal tail current measured at 100 μs after variable test

steps. The G-V curve was fit with the Boltzmann function to determine the potential for half-maximal activation (V_h) and apparent equivalent gating charge (z):

$$G(V) = \frac{G_{\max}}{1 + \exp\left(\frac{zF(V_h - V)}{RT}\right)} \quad (1)$$

Statistical analysis, graphing, and curve fitting were performed with OriginPro 7.5 (OriginLab Corporation, Northampton, MA). Nonlinear least squares fitting was based on the Levenberg-Marquardt algorithm. Mean values are presented as mean \pm S.E.M..

Chemicals

MTSET was obtained from Toronto Research Chemicals (North York, ON, Canada), dissolved in water at 100 mM and stored at -20 °C. Tetrabutylammonium nitrate (TBA) was obtained from Alfa Aesar (Ward Hill, MA). 1N KOH solution for pH adjustment was obtained from Fisher Scientific (Pittsburgh, PA). All other chemicals were purchased from Sigma-Aldrich (St. Louis, MO).

Results

Ag⁺ Inhibits BK Channel Activity At Nanomolar Concentrations

In an attempt to use Ag⁺ as a thiolate-reactive reagent to study the pore region of the mSlo1 BK channel, we found that Ag⁺ effectively eliminated BK activity at very low concentrations. As shown in Fig. 1A, 5 nM Ag⁺ silenced an inside-out patch containing hundreds of functional BK channels in less than 8 minutes. Such current reduction is not reversible during the time of our recordings. There was no hint of recovery even after the patch was washed in bath solution containing 10 mM dithiothreitol (DTT) for up to 20 minutes (Supplementary Fig. 1).

To measure the rate constant of this reaction, the patch membrane was held at -70 mV during reagent application. Macroscopic BK currents were evoked by brief 200-mV test pulses applied every second to monitor the reaction process. In Fig. 1B, the amplitudes of evoked BK currents (circles) are plotted against application time to show the course of modification of BK channels by Ag⁺. Usually there was a brief delay of 5-10 seconds before BK current began to decrease. The modification time course after this delay could be well fit with a single exponential function. For the patch shown in Fig. 1B, the exponential time constant is 3.84 s for modification by 520 nM Ag⁺. The modification rate was very sensitive to the solution exchange speed. Therefore, we routinely checked the solution exchange speed by switching between bath solutions containing 0 and 10 μM Ca²⁺ before Ag⁺ application (Fig. 1B, squares). For the patch shown in Fig.

1B, BK current reached a stable level within 1 second following the $[Ca^{2+}]$ jump. Data used in this study are all recorded from patches in which current reaches new steady-state level within 2 seconds upon the $[Ca^{2+}]$ jump.

The time constants of Ag^+ modification were measured at 5 concentrations spanning 5.2 to 520 nM (Fig. 1C). It should be noted that 5.2 nM Ag^+ , which was the lowest concentration we examined, is much lower than the proper buffering range of EDTA for Ag^+ . This might be the reason that the modification time constants with 5.2 nM Ag^+ show much larger deviation than those measured at higher concentrations, even though 5.2 nM Ag^+ readily eliminates BK channel activity. Assuming an irreversible bimolecular reaction mechanism for Ag^+ modification, the reaction rate constant can be calculated from the reciprocal of the exponential time constant. In Fig. 1D, the averaged Ag^+ blocking rates at the highest four Ag^+ concentrations (20, 52, 200, 520 nM) exhibit an approximate linear dependence on $[Ag^+]$. These four values were fit with a linear function to determine the second-order rate constant k , which is the slope of the fitted line. For $[Ag^+]$ from 20 to 520 nM, the average rate constant is $6.1 \times 10^5 M^{-1}s^{-1}$, which is orders of magnitude faster than the modification rate constants of methanethiosulfonate (MTS) reagents on cysteine residues on the C-terminus of the BK channel (Zhang and Horrigan, 2005), while also orders slower than the modification rate constant of Ag^+ on residues exposed in aquatic environment, such as those lining the ion permeation pathway of CNG channels (Contreras et al., 2008; Flynn and Zagotta, 2001).

Ag⁺ Inhibits BK Channel Activity By Modifying Cytosolically Accessible Residues

Next we examined whether Ag⁺ could also modify BK channels from the extracellular side. To do this we applied Ag⁺ on outside-out patches containing wild type BK channels. As shown in Fig. 2, there is no significant change of BK activity on an outside-out patch perfused in 520 nM Ag⁺ for 80 s. The amplitude of current only decreased by about 10% during the recording (Fig. 2B), which was indistinguishable from the spontaneous rundown of potassium current, which is often observed on excised patches in the absence of Ag⁺. Fig. 2C shows that normalized G-V curves are almost identical before (square) and after (circle) Ag⁺ application. Thus, key residue(s) for Ag⁺ modification must exist on the intracellular side of BK channel.

In the above experiments, Ag⁺ was applied to BK channels mainly in closed states (0 Ca²⁺, -70 mV). If the ion permeation gate of the BK channel is located at the intracellular end of ion permeation pathway, as suggested by the crystal structures of several potassium channels (Jiang et al., 2003; Long et al., 2005), then it might seem reasonable to assume that the target for Ag⁺ modification lies outside the ion permeation pathway. Two facts require further validation of this assumption. First, there is very limited information on the structure of the BK channels, including the location of BK channel ion permeation gate. Second, Ag⁺ readily diffuses through apertures with diameter of less than 5 Å (Flynn and Zagotta, 2001). Thus we performed several experiments to further assess the potential sites of Ag⁺ modification.

First we examined BK single channel activity in the presence of intracellular Ag^+ at single channel level. In Fig. 3A, two traces of single channel currents recorded before (gray) and during (black) the application of 52 nM Ag^+ are superimposed by their baselines. The activity of single BK channel is easily identified by the signature large single channel conductance of above 200 pS (Fig. 3B). It is clear that the single channel conductance was almost unchanged, though opening duration was dramatically reduced by Ag^+ modification. This result indicates that the ion permeation pathway of BK channels is intact during the modification by Ag^+ .

To further confirm that Ag^+ does not modify residues lining the ion permeation pathway of BK channels, we examined the effect of a cytosolic BK channel blocker on Ag^+ modification. The hypothesis is that, if Ag^+ attacked a residue lining the ion permeation pathway (including selectivity filter and central cavity), then a fast channel blocker should be able to hinder the access of Ag^+ to its target and thus slow down the modification. We chose TBA for this experiment because it is a well confirmed BK channel blocker with fast blocking kinetics (Li and Aldrich, 2004). Also, this blocker is commercially available in the form of nitrate and thus can co-exist with Ag^+ in nitrate-based solutions. During the experiment, the patch was first switched from control solution to solution containing 600 μM TBA for 10 s and then switched to solution containing both 600 μM TBA and 520 nM Ag^+ for modification (Fig. 4A). Upon switching to TBA solution, the BK channel current immediately dropped by about 50%, which agrees with a previous result that the IC_{50} of TBA is around 500 μM (Li and

Aldrich, 2004). However, the presence of TBA does not slow down the subsequent modification by Ag^+ . As shown in Fig. 4B, the mean time constant of modification in the presence of 600 μM TBA was almost identical to that without channel blocker.

The results from the above two experiments indicate that Ag^+ either does not modify residues lining the BK ion permeation pathway or the modification on these residues does not inhibit BK channel activity. However, these results do not exclude the possibility that Ag^+ inhibits BK channel activity by modifying residues in other regions of BK transmembrane segments. Thus we examined Ag^+ modification at a positive potential. We reasoned that, if the target of Ag^+ modification involves protein segments spanning the cell membrane, then the positively charged Ag^+ should sense transmembrane potential when accessing its target. Thus, positive membrane potential should accelerate the access of Ag^+ to its target and in turn increase its modification rate. However, we observed that Ag^+ modification rate is almost independent of membrane holding potential, as the modification time constant measured at 70 mV is almost identical to the one obtained at -70 mV (Fig. 5). This result suggests that the target for Ag^+ modification is not located in the transmembrane potential field.

Based on above observations, we conclude that the target for Ag^+ modification is a cytosolically accessible residue in the C-terminus or the intracellular linkers connecting transmembrane segments, but not those embedded in the cell membrane.

Ag⁺ Modifies Cysteines That Are Not Accessible To MTSET

Ag⁺, as a soft Lewis acid, forms a strong covalent bond with a soft Lewis base such as a thiolate group (Dance, 1986). Thus the 27 cysteines scattered on the intracellular side of the BK channels are the most promising candidates for Ag⁺ modification (Fig. 7A). Histidine is another possible target because a study on Shaker potassium channels showed that Cd²⁺, which is also a soft Lewis acid, coordinates with not only cysteine but also histidine (Holmgren et al., 1998). However, we found that Ag⁺ modification was not effected by pretreating BK channels with diethyl pyrocarbonate (DEPC), a reagent that modifies histidine residues (result not shown) (Means and Feeney, 1971). Since the hydrophilic histidine is unlikely to be buried deep inside the cytosolic structure of BK channel, we excluded histidines from further study and focused on cytosolic cysteines.

It has been reported that several MTS compounds, the most commonly used cysteine-modifying reagents, modify a common set of intracellular cysteines and change the gating behavior of BK channel (Zhang and Horrigan, 2005). Unlike Ag⁺, the effects of MTS reagents on BK gating are relatively weak as none of these reagents reduces the activity of BK channels completely. Some reagents, such as MTSET, even increase the activity of BK channels by negatively shifting the BK G-V relationship. We wondered whether residues modified by MTS reagents might overlap with those modified by Ag⁺.

We started with an MTSET protection experiment. In this experiment, we perfused inside-out patches in 200 μM MTSET for 3 minutes to completely modify BK channels (Zhang and Horrigan, 2005) before Ag⁺ application. As

shown in Fig. 6A, the G-V curve in 100 μM $[\text{Ca}^{2+}]_{\text{in}}$ is negatively shifted by more than 30 mV after MTSET treatment, which indicates that BK channels have been successfully modified. We then perfused the patch in 520 nM Ag^+ to see whether the MTSET pretreatment would protect the channels from being modified by Ag^+ . As shown in Fig. 6B and D, Ag^+ still effectively eliminated the activity of MTSET-modified BK channels at a rate comparable to that of control group. This result indicates that Ag^+ modifies at least one particular residue that is not accessible to MTSET, presumably because MTSET is bulkier than Ag^+ .

A previous study indicates that MTS reagents, including MTSET, sodium (2-sulfanatoethyl) methanethiosulfonate (MTSES) and N-ethylmaleimide (NEM), modify a shared set of cytosolic cysteine residues (Zhang and Horrigan, 2005). In addition, the modification by MTSES and NEM mainly inhibits the activity of BK channels. Thus we did not directly examine the protection of Ag^+ modification by these two reagents. To further confirm that the key residue of Ag^+ modification is different from those involved in MTS modification, we measured the modification rate of Ag^+ on the mSlo1 mutant C430S. Cys430 is a critical residue for the effects of MTS reagents on BK channels. When this cysteine is replaced by serine, the gating behavior of the resulting mutant is not altered by the treatment of MTS reagents (Zhang and Horrigan, 2005). However, as shown in Fig. 6 C and D, Ag^+ reduced the current of C430S at a rate identical to that of the wild type channels. This confirms that at least one key cysteine for Ag^+ modification is not available to MTSET and maybe other MTS reagents.

Multiple Critical Cysteines Are Involved In Ag⁺ Modification

As an attempt to identify the target of Ag⁺ modification on BK channels, we generated a series of cys-less constructs in which multiple cysteines were replaced by serines. Because some of the cytosolic cysteines are critical for the normal function of BK channel (Zhang and Horrigan, 2005; Tang et al., 2004), many of these constructs do not result in sufficient current for us to measure Ag⁺ modification in a Ca²⁺ free environment. However, one of these constructs, named mSlo1Cys6C, was robustly expressed in oocytes. In this construct, 1 extracellular cysteine in the N-terminus and 16 intracellular cysteines, including all 3 cysteines in S0-S1 linker and 13 out of 24 cysteines in the C-terminal tail are replaced by serines (Fig. 7A). The time course of modification of mSlo1Cys6C channels by 520 nM Ag⁺ is shown in Fig. 7B (inset, open squares). It is clear that the Ag⁺ modification of mSlo1Cys6C is much slower than of wild type channels (filled circles). The modification time constant averaged from 9 patches shows that the Ag⁺ modification rate is reduced by almost 20 times in this construct (Fig. 7B). This suggests that there are at least two key cysteines for Ag⁺ modification, one in the 16 intracellular cysteines that are mutated in Cys6C (group a: C2-4, C8-10, C20-25, C27-30), the other in the 11 intracellular cysteines that are still intact in Cys6C (group b: C7, C11-19, C26). Because mutations in group b usually result in non-functional or non-expressing channels, we did not attempt further identification of key residue in this group. Instead, we focused on the set of intracellular cysteines that have been substituted in Cys6C.

We further generated additional cys-less constructs in which a subset of cysteines in group a were replaced by serines. Only one of these constructs C20-25/27-30, in which the last 10 cysteines (C20-25, C27-30) were mutated into serines, shows reduced Ag^+ sensitivity. The Ag^+ modification rate on this construct is reduced by about 10 times when compared with that of wild type channels, but still two-fold faster than that of Cys6C (Fig. 7B). This suggests that there should be at least two key residues in group a, with one in the first 6 cysteines (group a1: C2-4, C8-10) and the other in the last 10 cysteines (group a2: C20-25, C27-30). Interestingly, the Ag^+ modification rate on construct C1-10, in which all 6 group a1 cysteines are replaced by serines, is identical to that wild type channels (Fig. 7B). This suggests that the modification effect of at least one C1-10 key residue can be compensated by the modification of another key residue outside the group.

For the 10 cysteines mutated in C20-25/27-30, we divided them into several subsets and generated corresponding cys-less constructs (C24/25/28/29, C26-29, C20, C21, C22, C23, C30). As shown in Fig. 7B, none of these constructs shows any significant reduction on Ag^+ sensitivity. We conclude that there are at least two key cysteines in group a2 that have at least partially identical effects on BK channel activity after being modified by Ag^+ .

As a summary, the results from above mutagenesis study suggest that there are at least four key cysteines (one in group a1, two in group a2 and one in group b) for Ag^+ modification on the intracellular side of BK channels. In addition, the effects of Ag^+ modification on some of these residues overlap with each other.

mSlo1Cys6C As A Potential Background For Studies of Ag⁺-accessibility

The fact that there are multiple key cysteines for Ag⁺ modification and the effects of Ag⁺ modification on these residues overlap with each other make it difficult to identify individual residues for Ag⁺ modification. However, in the course of this study we generated a cys-less construct Cys6C, in which the Ag⁺ modification rate is reduced by about 20-fold. In addition, as shown in Table 1 and Fig. 8 A and B, the G-V relationship of this construct is only moderately right-shifted in the presence of Ca²⁺ and is virtually identical to that of wild type channels in 0 Ca²⁺. Moreover, the activation and deactivation kinetics of this construct are also comparable to that of wild type channels (Fig. 8C, top traces). Furthermore, the construct still permits some Ca²⁺- and voltage-sensitive activity after Ag⁺ modification (Fig. 8D). Thus, Cys6C is a construct with reduced Ag⁺ sensitivity while retaining the normal gating behavior of BK channels. These properties, together with the fact that this construct exhibits robust expression in oocytes, suggest that Cys6C could be a valuable construct to probe Ag⁺ accessibility within the narrow regions of the BK channel pore.

Discussion

One of the most striking consequences of Ag^+ modification on wild type BK channels is that the modified channels seem almost completely inhibited, in contrast to the partial inhibition caused by some MTS reagents, such as MTSES and NEM (Zhang and Horrigan, 2005). The inhibitory effect of MTSES and NEM is mainly caused by a 5-fold decrease in the C-O equilibrium constant L of modified BK channels (Zhang and Horrigan, 2005). For Ag^+ modification, this essentially complete inhibition makes it difficult to assign the Ag^+ effect to a particular part of the BK channel activation mechanism. However, the data from mSlo1Cys6C provide clear evidence that at least part of the modification effect is to change the C-O equilibrium. As shown in Fig. 8C, there is still a considerable amount of residual current at the end of Ag^+ application to a patch expressing mSlo1Cys6C channels. The activation kinetics of this residual activity is much slower than that before Ag^+ treatment (Fig. 8E1). When fit with a single exponential function, the time constant of Cys6C activation before Ag^+ modification is 0.14 ms, which is comparable to that of the wild type channels. After Ag^+ modification, the activation time constant was increased by about 10 times to 1.4 ms. On the other hand, deactivation kinetics is relatively unaffected by Ag^+ modification (Fig. 8E2). The time constants of deactivation at -120 mV before and after Ag^+ modification are 0.23 ms and 0.26 ms respectively, both of which are close to that of wild type channels. This observation suggests that Ag^+ modification in mSlo1Cys6C slows the rate-limiting forward transitions of activation without altering the reverse transition of deactivation. Since voltage

sensor movements during activation are much faster than channel opening conformational steps (Horrigan and Aldrich, 1999), these effects on gating kinetics in 0 Ca^{2+} are consistent with the idea that Ag^+ modification reduces L of mSlo1Cys6C by about 10-fold, which is twice as much as that caused by MTS reagent modification (Zhang and Horrigan, 2005).

Two recently published crystal structures of the human BK channel intracellular gating ring (Wu et al., 2010; Yuan et al., 2010) may point to future approaches to the problem of BK channel inhibition caused by Ag^+ -modification. As shown in supplementary Fig. 2, the cytosolic domain of a single BK subunit contains two RCK sub domains, which interlock with each other at a flexible interface to form a bilobed dimer structure. Four such dimers then contact at the assembly interfaces (colored in cyan) to form the gating ring. The 23 cysteines in the cytosolic domain are colored in yellow. It can be seen that there are 9 cysteines, the sulfur of which is 10 Å within either of these two types of important interfaces. For example, C7, C8, C9, and C10 are close to the assembly interface in the RCK1 sub domain (Supplementary Fig. 2A); C19, C21 and C22 are close to the assembly interface in the RCK2 sub domain (Supplementary Fig. 2B); while C11 and C23 are close to the RCK1 helix-turn-helix structure that forms the flexible interface within a subunit (Supplementary Fig. 2B). Conceivably, modification of these residues by Ag^+ may disrupt these interfaces and cause the gating ring to collapse. Since the gating ring connects directly to the BK ion permeation pore, the collapse of the gating ring may lock the BK pore in a closed conformation, perhaps somewhat different from normal closed conformations in

that Ag^+ modified closed channels cannot be opened by either depolarization or elevated $[\text{Ca}^{2+}]_{\text{in}}$. It should be noted that 6 of these 9 cysteines are replaced by alanines in mSlo1Cys6C and thus do not account for Ag^+ -mediated inhibition in this construct. However, 3 of them (C7, C11 and C19) resulted in non-functional or non-expressing channels once mutated and thus were intact in mSlo1Cys6C. It is interesting to consider that Ag^+ attack of these residues may produce BK channel inhibition in a fashion similar to mutations of these same residues.

The strong inhibition of Ag^+ on BK channels raises the question whether such inhibition could contribute to silver cytotoxicity. As a widely distributed element, silver compounds can be absorbed in humans from a variety of sources, including air, drinking water, and silver-based medical supplies such as arthroplasty cement and topical wound agents (Chopra, 2007; Vik et al., 1985). Once absorbed, silver accumulations are found in myocardium, mucous membrane, kidney, liver, and many areas of the brain (Iwasaki et al., 1997; Dietl et al., 1984). It has been revealed by an autometallographic (AMG) silver method that Ag^+ may penetrate through cell membranes and accumulate inside cells, even forming deposits in neurons behind the blood-brain barrier (Stoltenberg et al., 1994; Rungby, 1990; Pelkonen et al., 2003). Given the similar size between Ag^+ and physiological cations such as Na^+ and K^+ , there are several possible routes for Ag^+ entry into cell membrane. First, Ag^+ might permeate through cell membranes via various ion channels (Bury and Wood, 1999). It has been reported that Ag^+ is able to enter the branchial apical membrane of rainbow trout via the proton-coupled Na^+ channel (Bury and Wood, 1999). Second, Ag^+ may

also be taken up by transporters such as the copper transporter Ctr1 (Petris et al., 2003). In any case, the extracellular $[Ag^+]$ is likely to be very low because of relatively high extracellular $[Cl^-]$ (100 mM (Hille, 2001)) and low AgCl solubility (solubility product: $1.6 \times 10^{-10} M^2$ (Brady and Senese, 2007)). However, for the case of permeation through ion channels, it only requires 0.3 nM extracellular $[Ag^+]$ to obtain 5 nM intracellular $[Ag^+]$ at a negative resting potential of -75 mV. The existence of active transport mechanisms may further facilitate the cytosolic accumulation of Ag^+ .

Since BK channels are widely distributed in excitatory and non-excitatory cells and participate in many important physiology processes, irreversible modification of BK channels by Ag^+ could be an important cellular event underlying silver toxicity. Several published results suggest that this is not an unreasonable hypothesis. First, silver is found to accumulate in BK-expressing organs and tissues, such as vascular smooth muscle, kidney, and cerebellum (Ghatta et al., 2006;Pelkonen et al., 2003). Second, symptoms resulted from acute intoxication with large doses of Ag^+ include diarrhea, cardiovascular collapse and convulsions (Dreisbach, 1974), conditions which might be expected to arise from BK channel inhibition (Hagen et al., 2003;Sheehan et al., 2009). Finally, both Ag^+ treatment and BK channel gene knockout induce neuron degeneration (Wachter et al., 2002;Ruttiger et al., 2004). Though more work will be required before a clear connection between silver toxicity and irreversible modification of BK channels by Ag^+ can be made, our results, together with these previous findings, suggest that more attention be paid to the potential cytotoxicity of Ag^+ .

In summary, our study shows that intracellular Ag^+ at nanomolar concentrations irreversibly blocks the activation of wild type BK channels. The modification of at least four cytosolic cysteines by Ag^+ is involved in this inhibition. At least one of these key cysteines is not accessible to the bulkier thiolate reagent MTSET, and thus may not be exposed on the surface of the BK protein. A partial cys-less construct generated in this study shows reduced Ag^+ sensitivity and normal gating behavior and thus could be used as a background channel when Ag^+ is required to probe the structure of BK channel. Though more work will be required to establish a firm relationship between Ag^+ -inhibition of BK channels and Ag^+ related cytotoxicity, our results point to BK channels as a potential contributing factor in silver cytotoxicity. More importantly, our results suggest caution in regards to the medical use of silver compounds.

Acknowledgements

We thank Yefei Cai for technical assistance. We thank Dr. Steven L. Brody for his valuable comments concerning Ag⁺ uptake mechanisms.

References

Bayston R, Mills A, Howdle S M and Ashraf W (2007) Comment on: the Increasing Use of Silver-Based Products As Antimicrobial Agents: a Useful Development or a Cause for Concern? *J Antimicrob Chemother* 60:447-448.

Brady JE and Senese F (2007) *Chemistry: Matter and Its Changes*. Wiley.

Bury NR and Wood C M (1999) Mechanism of Branchial Apical Silver Uptake by Rainbow Trout Is Via the Proton-Coupled Na(+) Channel. *Am J Physiol* 277:R1385-R1391.

Butler A, Tsunoda S, McCobb D P, Wei A and Salkoff L (1993) MSlo, a Complex Mouse Gene Encoding "Maxi" Calcium-Activated Potassium Channels. *Science* 261:221-224.

Chopra I (2007) The Increasing Use of Silver-Based Products As Antimicrobial Agents: a Useful Development or a Cause for Concern? *J Antimicrob Chemother* 59:587-590.

Contreras JE, Srikumar D and Holmgren M (2008) Gating at the Selectivity Filter in Cyclic Nucleotide-Gated Channels. *Proc Natl Acad Sci U S A* 105:3310-3314.

Dance IG (1986) The Structural Chemistry of Metal Thiolate Complexes. *Polyhedron* 5:1037-1104.

Danscher G (1981) Light and Electron Microscopic Localization of Silver in Biological Tissue. *Histochemistry* 71:177-186.

del Camino D and Yellen G (2001) Tight Steric Closure at the Intracellular Activation Gate of a Voltage-Gated K(+) Channel. *Neuron* 32:649-656.

Dietl HW, Anzil A P and Mehraein P (1984) Brain Involvement in Generalized Argyria. *Clin Neuropathol* 3:32-36.

Dreisbach RH (1974) *Handbook of Poisoning: Diagnosis & Treatment*. Lange Medical Publications, Los Altos, CA.

Flynn GE and Zagotta W N (2001) Conformational Changes in S6 Coupled to the Opening of Cyclic Nucleotide-Gated Channels. *Neuron* 30:689-698.

Ghatta S, Nimmagadda D, Xu X and O'Rourke S T (2006) Large-Conductance, Calcium-Activated Potassium Channels: Structural and Functional Implications. *Pharmacol Ther* 110:103-116.

Hagen BM, Bayguinov O and Sanders K M (2003) Beta 1-Subunits Are Required for Regulation of Coupling Between Ca²⁺ Transients and Ca²⁺-Activated K⁺ (BK) Channels by Protein Kinase C. *Am J Physiol Cell Physiol* 285:C1270-C1280.

Hamill OP, Marty A, Neher E, Sakmann B and Sigworth F J (1981) Improved Patch-Clamp Techniques for High-Resolution Current Recording From Cells and Cell-Free Membrane Patches. *Pflugers Arch* 391:85-100.

Hille B (2001) *Ion Channels of Excitable Membranes*. Sinauer, Sunderland, Mass.

Holmgren M, Shin K S and Yellen G (1998) The Activation Gate of a Voltage-Gated K⁺ Channel Can Be Trapped in the Open State by an Intersubunit Metal Bridge. *Neuron* 21:617-621.

Horrigan FT and Aldrich R W (1999) Allosteric Voltage Gating of Potassium Channels II. Mslo Channel Gating Charge Movement in the Absence of Ca(2+). *J Gen Physiol* 114:305-336.

Hultberg B, Andersson A and Isaksson A (1997) Copper Ions Differ From Other Thiol Reactive Metal Ions in Their Effects on the Concentration and Redox Status of Thiols in HeLa Cell Cultures. *Toxicology* 117:89-97.

Iwasaki S, Yoshimura A, Ideura T, Koshikawa S and Sudo M (1997) Elimination Study of Silver in a Hemodialyzed Burn Patient Treated With Silver Sulfadiazine Cream. *Am J Kidney Dis* 30:287-290.

Jiang Y, Lee A, Chen J, Ruta V, Cadene M, Chait B T and MacKinnon R (2003) X-Ray Structure of a Voltage-Dependent K⁺ Channel. *Nature* 423:33-41.

Li M, Chang T H, Silberberg S D and Swartz K J (2008) Gating the Pore of P2X Receptor Channels. *Nat Neurosci* 11:883-887.

Li W and Aldrich R W (2004) Unique Inner Pore Properties of BK Channels Revealed by Quaternary Ammonium Block. *J Gen Physiol* 124:43-57.

Long SB, Campbell E B and MacKinnon R (2005) Crystal Structure of a Mammalian Voltage-Dependent Shaker Family K⁺ Channel. *Science* 309:897-903.

Means GE and Feeney R E (1971) *Chemical Modification of Proteins*. Holden-Day, San Francisco.

Payne CM, Bladin C, Colchester A C, Bland J, Lapworth R and Lane D (1992) Argyria From Excessive Use of Topical Silver Sulphadiazine. *Lancet* 340:126.

Pelkonen KH, Heinonen-Tanski H and Hanninen O O (2003) Accumulation of Silver From Drinking Water into Cerebellum and Musculus Soleus in Mice. *Toxicology* 186:151-157.

Petris MJ, Smith K, Lee J and Thiele D J (2003) Copper-Stimulated Endocytosis and Degradation of the Human Copper Transporter, HCtr1. *J Biol Chem* 278:9639-9646.

Rungby J (1990) An Experimental Study on Silver in the Nervous System and on Aspects of Its General Cellular Toxicity. *Dan Med Bull* 37:442-449.

Rungby J, Slomianka L, Danscher G, Andersen A H and West M J (1987) A Quantitative Evaluation of the Neurotoxic Effect of Silver on the Volumes of the Components of the Developing Rat Hippocampus. *Toxicology* 43:261-268.

Russell AD and Hugo W B (1994) Antimicrobial Activity and Action of Silver. *Prog Med Chem* 31:351-370.

Ruttiger L, Sausbier M, Zimmermann U, Winter H, Braig C, Engel J, Knirsch M, Arntz C, Langer P, Hirt B, Muller M, Kopschall I, Pfister M, Munkner S, Rohbock K, Pfaff I, Rusch A, Ruth P and Knipper M (2004) Deletion of the Ca²⁺-Activated Potassium (BK) Alpha-Subunit but Not the BKbeta1-Subunit Leads to Progressive Hearing Loss. *Proc Natl Acad Sci U S A* 101:12922-12927.

Sheehan JJ, Benedetti B L and Barth A L (2009) Anticonvulsant Effects of the BK-Channel Antagonist Paxilline. *Epilepsia* 50:711-720.

Stoltenberg M, Juhl S, Poulsen E H and Ernst E (1994) Autometallographic Detection of Silver in Hypothalamic Neurons of Rats Exposed to Silver Nitrate. *J Appl Toxicol* 14:275-280.

Tang XD, Garcia M L, Heinemann S H and Hoshi T (2004) Reactive Oxygen Species Impair Slo1 BK Channel Function by Altering Cysteine-Mediated Calcium Sensing. *Nat Struct Mol Biol* 11:171-178.

Vik H, Andersen K J, Julshamn K and Todnem K (1985) Neuropathy Caused by Silver Absorption From Arthroplasty Cement. *Lancet* 1:872.

Wachter BG, Leonetti J P, Lee J M, Wurster R D and Young M R (2002) Silver Nitrate Injury in the Rat Sciatic Nerve: a Model of Facial Nerve Injury. *Otolaryngol Head Neck Surg* 127:48-54.

Wagner PA, Hoekstra W G and Ganther H E (1975) Alleviation of Silver Toxicity by Selenite in the Rat in Relation to Tissue Glutathione Peroxidase. *Proc Soc Exp Biol Med* 148:1106-1110.

Wu Y, Yang Y, Ye S and Jiang Y (2010) Structure of the Gating Ring From the Human Large-Conductance Ca(2+)-Gated K(+) Channel. *Nature*.

Xia XM, Zeng X and Lingle C J (2002) Multiple Regulatory Sites in Large-Conductance Calcium-Activated Potassium Channels. *Nature* 418:880-884.

MOL #66407

Yuan P, Leonetti M D, Pico A R, Hsiung Y and MacKinnon R (2010) Structure of the Human BK Channel Ca²⁺-Activation Apparatus at 3.0 Å Resolution. *Science*.

Zhang G and Horrigan F T (2005) Cysteine Modification Alters Voltage- and Ca²⁺-Dependent Gating of Large Conductance (BK) Potassium Channels. *J Gen Physiol* 125:213-236.

Zhang X, Solaro C R and Lingle C J (2001) Allosteric Regulation of BK Channel Gating by Ca²⁺ and Mg²⁺ Through a Nonselective, Low Affinity Divalent Cation Site. *J Gen Physiol* 118:607-636.

Footnotes

This work was supported by the National Institutes of Health National Cancer Institute [Grant GM66315].

Legends for Figures

Fig. 1. Ag^+ irreversibly eliminates the activity of BK channels at nanomolar concentrations. A, BK currents evoked by 200 mV test pulses in 0-Ca^{2+} solution before (gray) and after (black) 8-min perfusion in 5.2 nM Ag^+ . The upper trace shows the test protocol. The transient capacitive currents increased during Ag^+ treatment because the recording pipette was increasingly submerged in bath during perfusion. B, The time course of Ag^+ modification on BK channels. The solution exchange speed was measured before Ag^+ modification by switching the patch between 0-Ca^{2+} and $10\ \mu\text{M}\ \text{Ca}^{2+}$. To monitor the change of BK open probability, membrane potential was briefly (3-ms) stepped to 200 mV from holding potential of 70 mV at a frequency of 1 Hz. Each square on the plot is the mean value of the last 50 sampling points of current evoked by each test pulse. It is clear that new $[\text{Ca}^{2+}]_{\text{in}}$ was reached within 1 s on this patch (squares). The time course of Ag^+ modification (circles) was determined by the same voltage protocol. Ag^+ application started at $t = 13\ \text{s}$ and ended at $t = 46\ \text{s}$. The solid line is the single-exponential fit to the modification time course. All time course plots of Ag^+ modification in this paper were constructed in a similar way. The inset on the right shows sample currents before (5th), at the beginning (14th), in the middle (18th), and near the end (40th) of modification. C, The time constants of Ag^+ modification are plotted against free Ag^+ concentration. The lines connecting the data points have no physical meaning. (D) The reciprocals of modification time constants are plotted against free Ag^+ concentration. The values at the highest four concentrations (filled circles) were linearly fit to determine the rate constant

of Ag^+ modification, which is the slope of the solid line. The value at 5.2 nM Ag^+ (open circle) is not included in this fit. It is worth mentioning that the fitting gives a slightly increased k of $8.5 \times 10^5 \text{ M}^{-1}\text{s}^{-1}$ with Pearson's correlation coefficient of 0.96 when all five values are included, which suggests that the modification by 5 nM Ag^+ is not derived from the postulated linear relationship.

Fig. 2. Extracellular Ag^+ does not modify BK channels. A, Macroscopic BK currents before (bottom left) and after (right) the application of 520 nM Ag^+ were recorded from an outside-out patch. The voltage protocol is shown in the top of left panel. Pipette solution (intracellular side) contained 1 μM Ca^{2+} . B, Time course of Ag^+ modification. The patch was perfused in 520 nM Ag^+ for 80 seconds. The slight decrease of current was probably caused by rundown. C, The G-V profiles of macroscopic BK currents before (square) and after (circle) Ag^+ treatment are shown. The lines are the fit of the Boltzmann function. The results are: before Ag^+ perfusion, $V_h = 146 \text{ mV}$, $z = 0.87$ (gray trace), after Ag^+ perfusion, $V_h = 143 \text{ mV}$, $z = 0.85$ (black trace).

Fig. 3. Ag^+ modification does not change BK single channel conductance. A, Sample traces of BK single channel activity before (gray, dotted) and during (black, solid) the application of 52 nM Ag^+ . The patch was held at -70 mV . A 50-ms depolarizing pulse to 140 mV was given each second to activate BK channels. Closed and open levels of BK activity are marked by dashed lines. The two brief openings during Ag^+ modification are circled by dotted lines. B, The single

channel conductance of BK channel was plotted against time. Each point is the mean single channel conductance of opening events evoked by a 140 mV test pulse. The single channel conductance averaged from 20 traces before Ag^+ application is 240 ± 2.2 pS, the single channel conductance averaged from 19 traces during Ag^+ modification is 236 ± 2.2 pS. The gray line shows the time course of macroscopic modification by 52 nM Ag^+ .

Fig. 4. The modification rate by Ag^+ on BK current is not altered in the presence of channel blocker. A, Time course of BK modification by 520 nM Ag^+ in the presence of 600 μM TBA. The patch was first perfused in 600 μM TBA for 10 seconds and then switched to a solution containing both TBA and 520 nM Ag^+ for modification. B, The histogram of mean modification time constants by 520 nM Ag^+ with 0 (3.5 ± 0.8 s, $n = 6$) or 600 μM (3.01 ± 1.05 s, $n = 6$) TBA.

Fig. 5. The modification of BK channels by Ag^+ at positive potential. A, Macroscopic currents evoked by 200 mV test pulses in 0- Ca^{2+} solution before (gray) and after (black) perfusion in 200 nM Ag^+ . The holding potential was 70 mV. B, Time course of Ag^+ modification of BK channels at 70 mV. The Ag^+ concentration was 200 nM. The modification started at the 17th second and ended at 90th second. C, The histogram of mean modification time constants by 200 nM Ag^+ at -70 (6.7 ± 1.3 s, $n = 6$) or 70 mV (6.8 ± 1.2 s, $n = 4$).

Fig. 6. The targets for Ag^+ modification are different from those for MTS reagents. A, The G-V profile of macroscopic BK currents in $100 \mu\text{M} [\text{Ca}^{2+}]_{\text{in}}$ before (black square) and after (gray circle) perfused in $200 \mu\text{M}$ MTSET for 3 minutes. The Boltzmann fitting results are: $V_h = 27 \text{ mV}$, $z = 1.14$ (before); $V_h = -8 \text{ mV}$, $z = 1.22$ (after). B, The time course of modification on BK channels by 520 nM Ag^+ after MTSET treatment. Modification started at $t = 29 \text{ s}$ and ended at $t = 60 \text{ s}$. C, The time course of modification on mSlo1C430S by 520 nM Ag^+ . Modification started at $t = 20 \text{ s}$ and ended at $t = 70 \text{ s}$. D, The histogram of mean modification time constants by 520 nM Ag^+ on BK currents ($3.5 \pm 0.8 \text{ s}$, $n = 6$), BK currents after MTSET application ($2.92 \pm 0.3 \text{ s}$, $n = 3$), and mSlo1C430S currents ($3.7 \pm 0.6 \text{ s}$, $n = 4$).

Fig. 7. Ag^+ sensitivity of various cys-less constructs. A, The schema maps the linear distribution of 30 cysteines on the BK channel. Upper row is the cysteines on the extracellular side and in the transmembrane segments of BK channel. Bottom row is the cysteines in the cytosolic domain. Three extracellular cysteines are marked by bars above squares. The number in each square refers to the sequential number of that cysteine. The numbers above squares are the actual positions of cysteines in mSlo1. In mSlo1Cys6C, 17 of these cysteines are mutated into serines (shaded). B, The mean modification time constants of various cys-less constructs by 520 nM Ag^+ : wild type ($3.5 \pm 0.8 \text{ s}$, $n = 6$), Cys6C ($61 \pm 6.6 \text{ s}$, $n = 9$), C1-4 ($3.9 \pm 0.6 \text{ s}$, $n = 5$), C1-10 ($3.2 \pm 0.45 \text{ s}$, $n = 6$), C20-25/27-30 ($30.8 \pm 4.5 \text{ s}$, $n = 8$), C24/25/28/29 ($2.7 \pm 0.2 \text{ s}$, $n = 6$), C26-29 ($2.7 \pm$

0.5 s, n = 4), C20 (2.3 ± 0.4 s, n = 5), C21 (2.1 ± 0.2 s, n = 4), C22 (2.64 ± 0.28 s, n = 5), C23 (3.2 ± 0.97 s, n = 4), C30 (2.2 ± 0.3 s, n = 4). Only Cys6C and C20-25/27-30 show significantly reduced Ag^+ sensitivity, as marked by *. Inset, The time course of modification on mSlo1Cys6C (open square) by 520 nM Ag^+ overlapped with that of wild type BK (filled circle) at the beginning of Ag^+ application, as indicated by time 0.

Fig. 8. Gating behavior and Ag^+ sensitivity of mSlo1Cys6C. A, The G-V curves of mSlo1Cys6C (filled symbols) in a wide range of $[\text{Ca}^{2+}]_{\text{in}}$ overlap with those of mSlo1 (open symbols) in various $[\text{Ca}^{2+}]_{\text{in}}$ (in μM): 0(square), 1(circle), 10(triangle), 100(diamond), 300(star). Each set of data is averaged from 5 patches. Lines are Boltzmann fits. B, The V_h s of mSlo1Cys6C and BK channels are plotted against $[\text{Ca}^{2+}]_{\text{in}}$ (in log scale). The connecting lines have no physical meaning. C, Macroscopic mSlo1Cys6C currents recorded in 100 μM $[\text{Ca}^{2+}]_{\text{in}}$ before (top) and after (bottom) 240-sec perfusion in 520 nM Ag^+ . The voltage protocol was similar to the one used in the panel A of Fig. 2. Notice the time scales are different in these two sets of recordings. D, The macroscopic G-V profiles of mSlo1Cys6C in 100 μM Ca^{2+} before Ag^+ modification (filled circle), and in 10 μM (open star) and 100 μM $[\text{Ca}^{2+}]_{\text{in}}$ (open circle) after Ag^+ modification. The Boltzmann fitting results are: $V_h = 30$ mV, $z = 1.02$ (100 μM Ca^{2+} before Ag^+ treatment); $V_h = 150$ mV, $z = 0.88$ (10 μM Ca^{2+} after Ag^+ treatment); $V_h = 106$ mV, $z = 0.74$ (100 μM Ca^{2+} after Ag^+ treatment). E, Normalized activation (E1, 200 mV) and deactivation (E2, -120

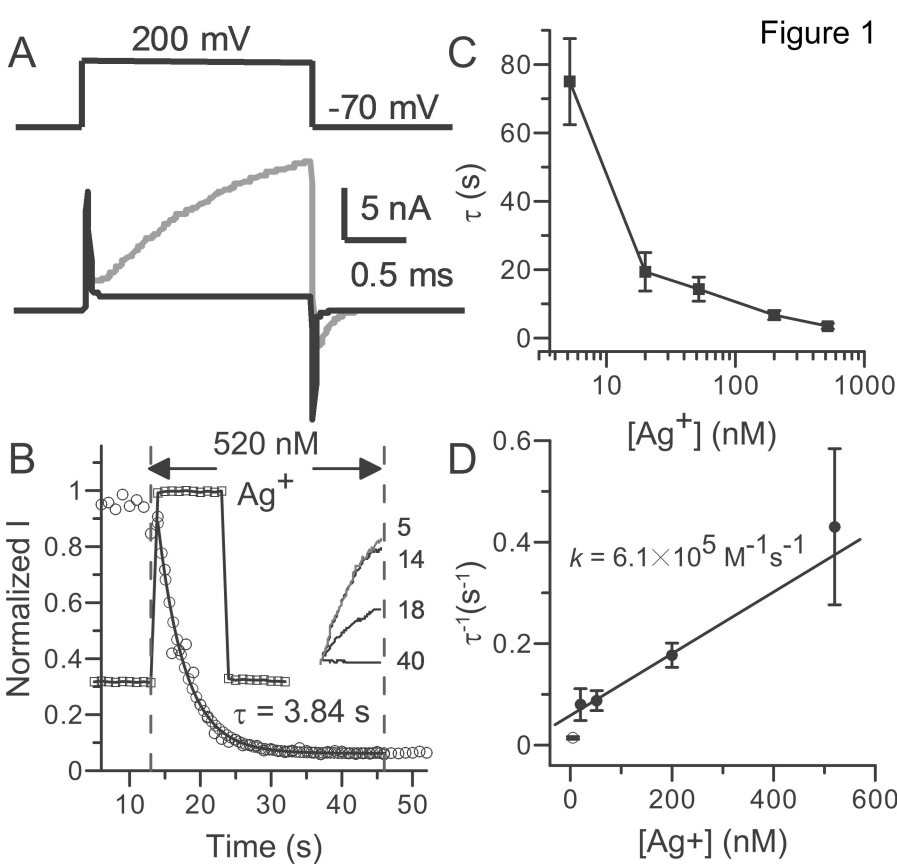
MOL #66407

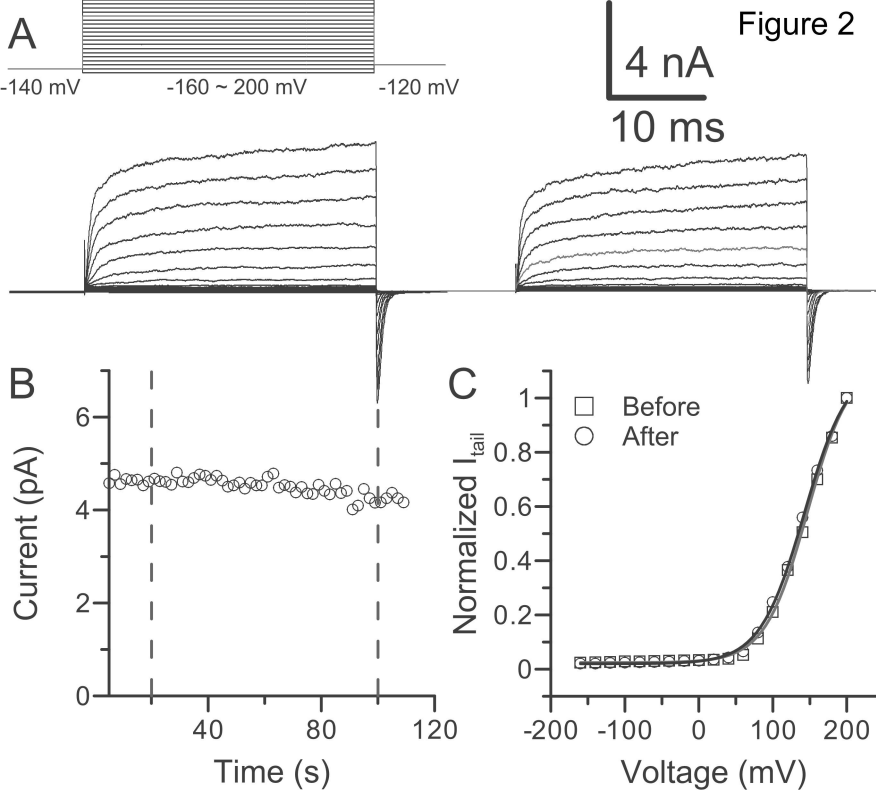
mV) time course of mSlo1Cys6C currents before (gray) and after (black) Ag⁺ modification.

Tables

Table 1: Boltzmann fitting results of the G-V relationships of mSlo1Cys6C and mSlo1 BK channels:

[Ca ²⁺] _{in}	mSlo1		mSlo1Cys6C	
	V _h (mV)	z	V _h (mV)	z
0 μM	206 ± 6.3	0.9 ± 0.03	210 ± 3.4	1.1 ± 0.02
1 μM	152 ± 5.8	0.9 ± 0.06	192 ± 4.2	1.1 ± 0.05
10 μM	58 ± 4.1	1.2 ± 0.13	72 ± 7.0	1.2 ± 0.07
100 μM	2 ± 3.3	1.4 ± 0.04	26 ± 6.1	1.4 ± 0.03
300 μM	-15 ± 3.1	1.2 ± 0.07	2.8 ± 4.1	1.2 ± 0.07





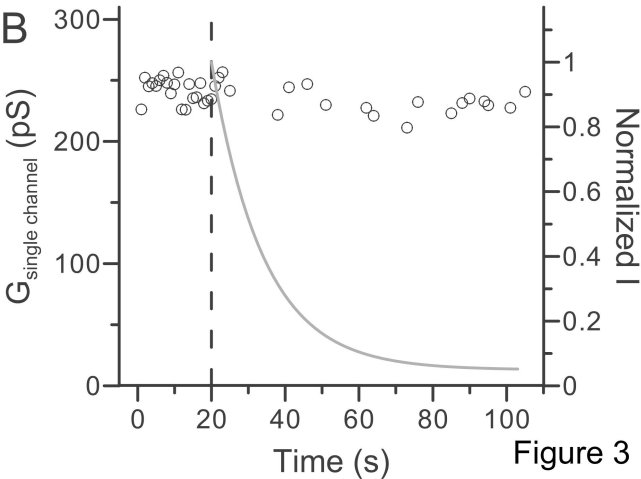
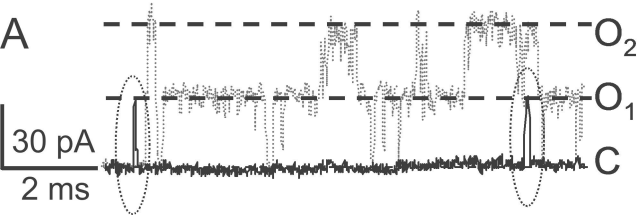
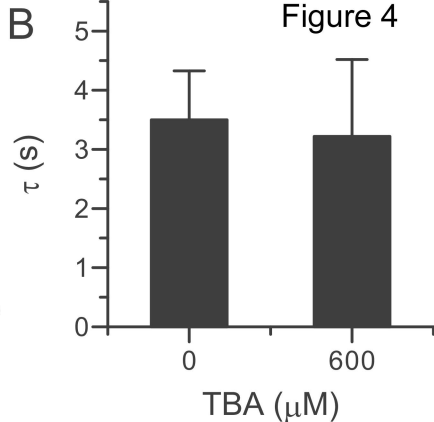
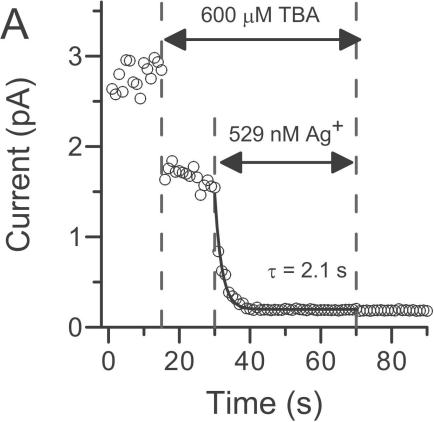
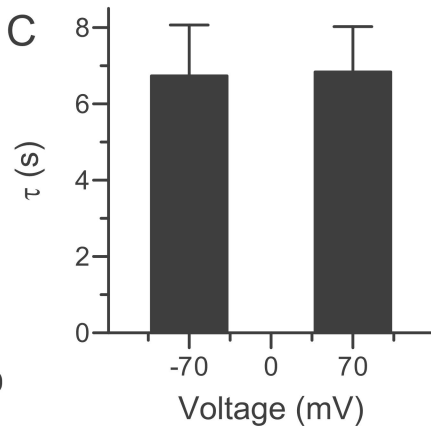
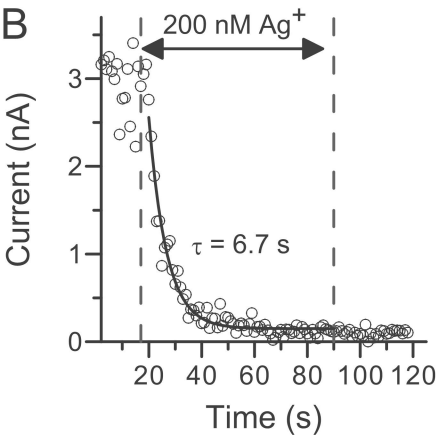
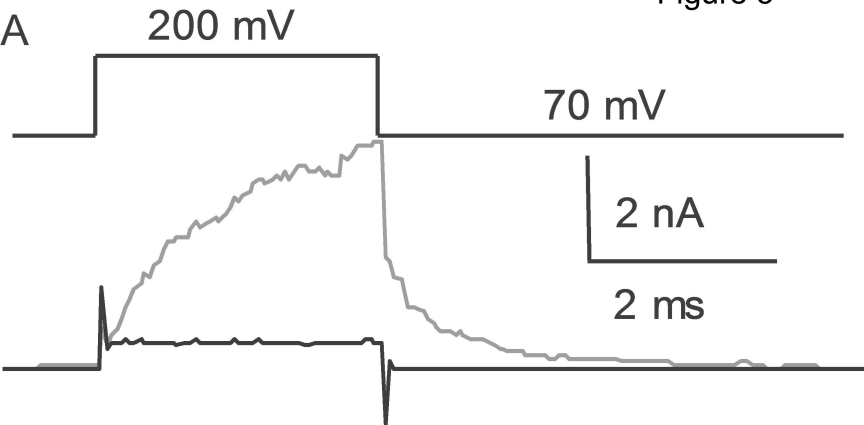


Figure 3





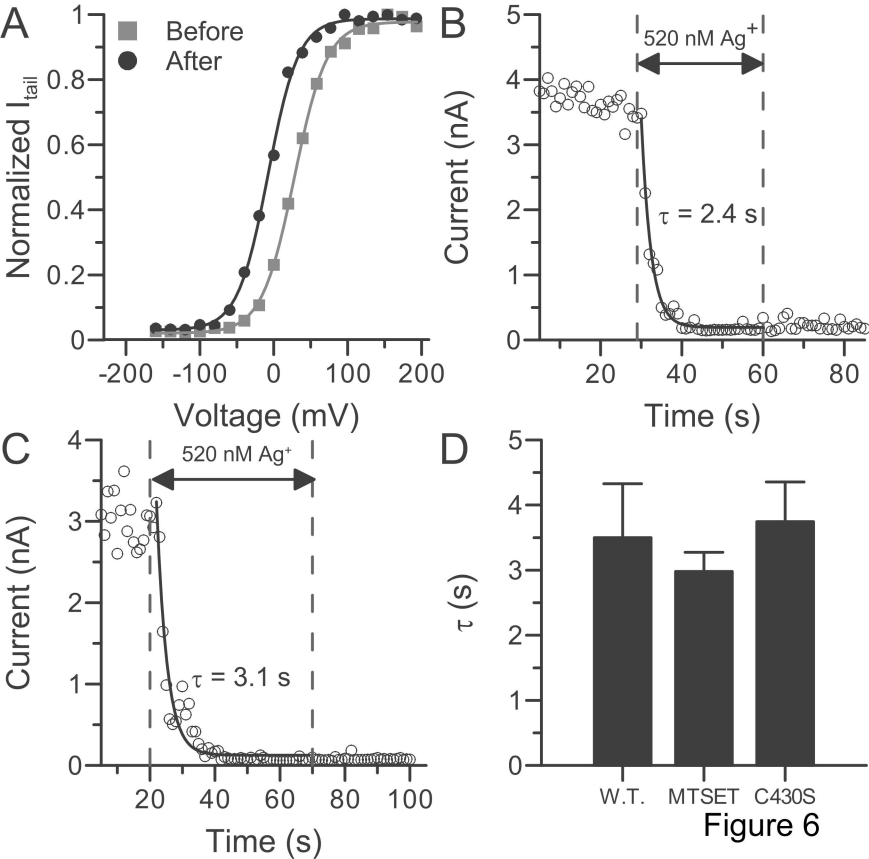
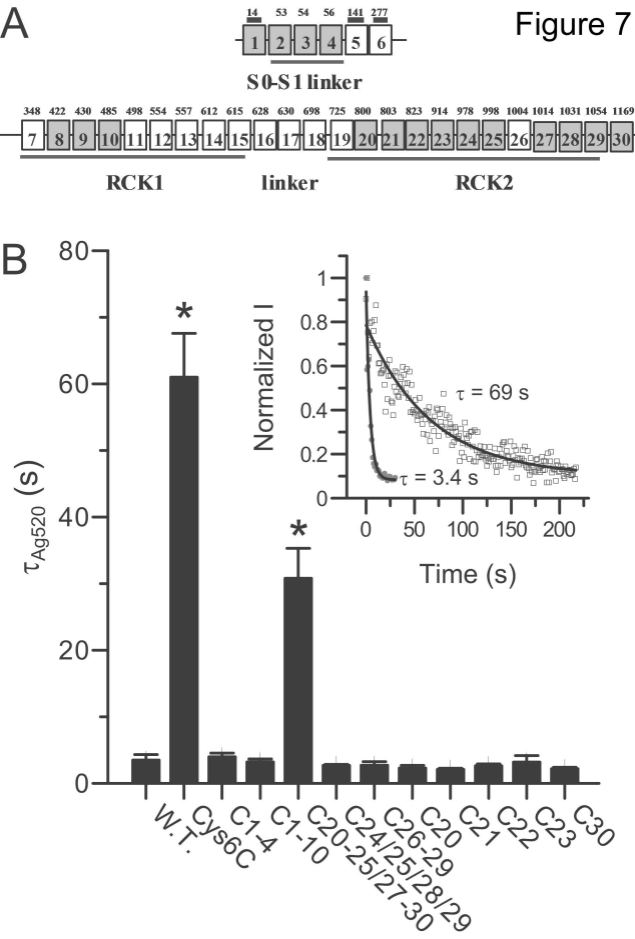
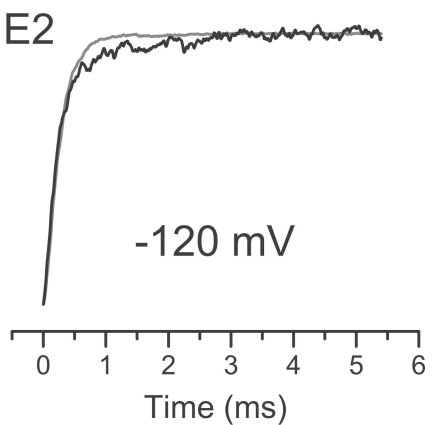
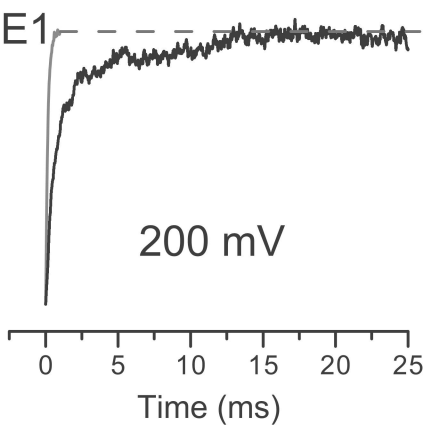
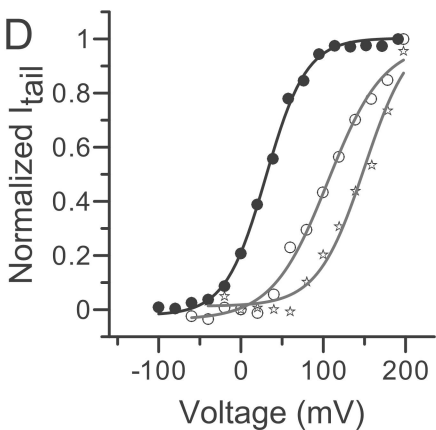
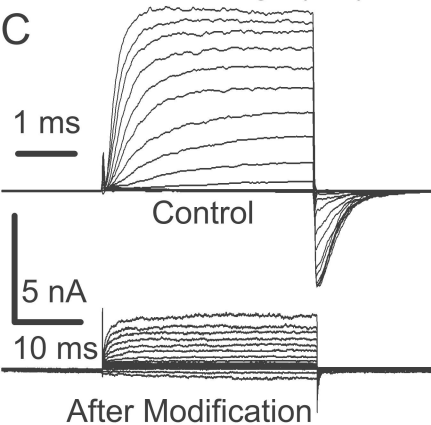
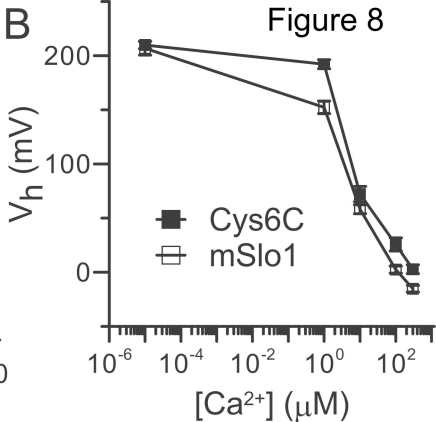
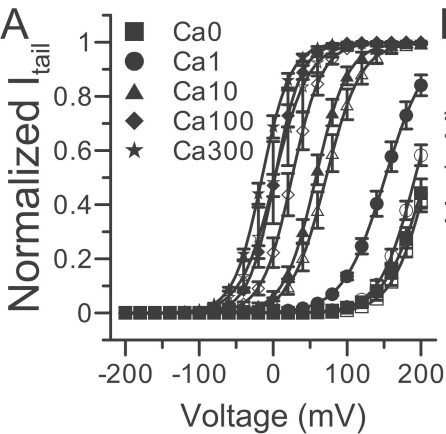


Figure 7





Journal: Molecular Pharmacology

Title: Inhibition of BK channels by nanomolar concentrations of Ag^+

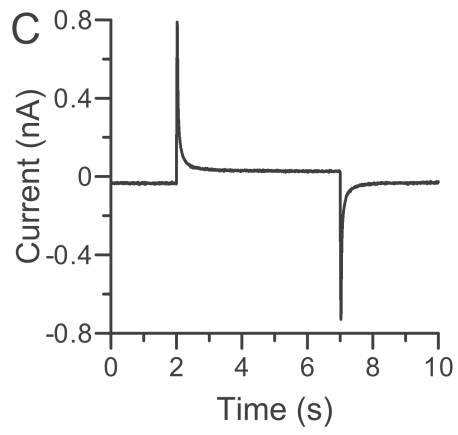
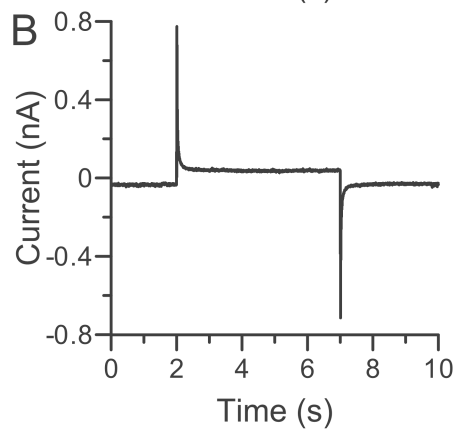
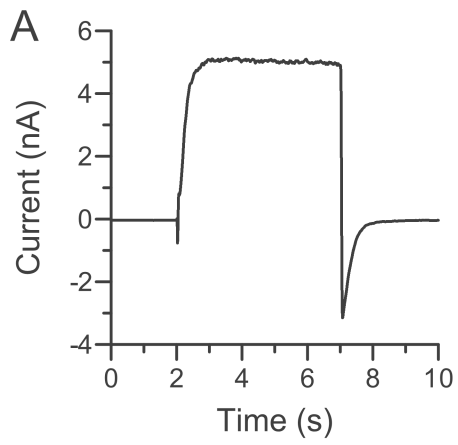
Authors: Yu Zhou, Xiaoming Xia, Christopher J. Lingle

Supplementary Fig. 1. Ag^+ inhibition cannot be reversed by DTT. A, BK current evoked by 200 mV test pulse in $10 \mu\text{M Ca}^{2+}$ before Ag^+ treatment. B, Current trace evoked by 200 mV test pulse in $10 \mu\text{M Ca}^{2+}$ after 2-min perfusion in 500 nM Ag^+ . C, Current trace evoked by 200 mV test pulse in $10 \mu\text{M Ca}^{2+}$ after 20-min perfusion in 10 mM DTT.

Supplementary Fig. 2. Distribution of cysteines in the cytosolic domain of a BK α -subunit. The structural pictures are rendered from the Ca^{2+} -free human BK cytosolic domain structure (Protein Data Bank id: 3NFA) in UCSF Chimera (<http://www.cgl.ucsf.edu/chimera/>). The linker between the cytosolic domain and the BK pore is colored in white. The RCK1 sub domain is colored in blue. The RCK2 sub domain is colored in red. The two assembly interfaces are colored in cyan. The intermediate helix-turn-helix structures in RCK1 and RCK2 that form the flexible interface are colored in cornflower blue and magenta, respectively. The Ca^{2+} -bowl is colored in orange. Cysteines are colored in yellow. The numbers in parentheses are the residue sequence numbers of cysteines in mSlo1. A, The structure is oriented to show the cysteines (C7, C8, C9, C10) near the assembly interface in the RCK1 sub domain. The side chains of these 4 cysteines are displayed as ball-stick. B, The structure is oriented to show the

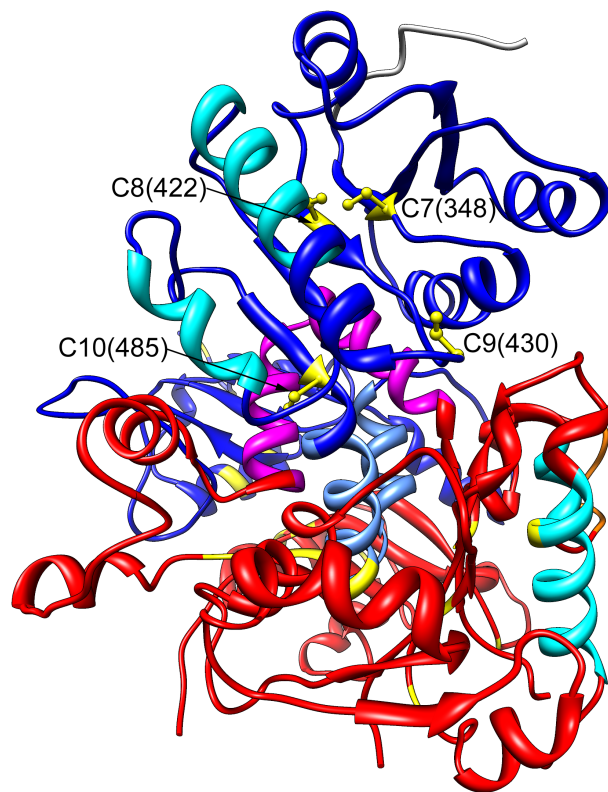
cysteines near the flexible interface (C11 and C23) or the RCK2 assembly interface (C19, C21 and C22). The side chains of these 5 cysteines are displayed as ball-stick.

Supplementary Fig. 1



Supplementary Fig. 2

A



B

